

A STUDY ON IMPACT OF BAND-TO-BAND MISREGISTRATION ON ASTER TIR PRODUCTS

Hideyuki Tonooka¹, and Tomoharu Muneta²

¹ Associate Professor, ² Graduate Student, ^{1,2} Ibaraki University, Japan

¹ Phone: +81-294-38-5292, ¹ Fax: +81-294-38-5158, ¹ tonooka@mx.ibaraki.ac.jp

KEY WORDS: Emissivity, Level-1 processing, Geometric correction, GCP, Stripe noise

ABSTRACT

The Advanced Spaceborne Thermal Emission and Reflection Radiometer (ASTER) onboard the NASA's Terra satellite has five spectral bands (bands 10 to 14) in the thermal infrared (TIR) spectral region (8 to 12 μm) with a spatial resolution of 90 m. These TIR bands can be used for retrieval of both land surface temperature and spectral emissivity which are delivered to users as standard products. Surface emissivity retrieval is sensitive to input radiance errors, and it is known that some of ASTER emissivity products, particularly resampled by the nearest neighbor (NN) method, include significant stripe noises. The present study focuses on the impact of band-to-band misregistration on emissivity products. We compare surface emissivity images retrieved from a level-1B product resampled by NN, a level-1A product, a level-3A product resampled by NN, a level-1A product geolocated by NN using a common ground-control-point (GCP) table, and a level-1A product geolocated by NN using the GCP table of each band. The results indicate that some of level-1B and -3A products resampled by NN will give stripe noises to emissivity products probably due to some mismatch in GCP tables among bands. We also suggest a geolocation approach for reducing such misregistration.

1. INTRODUCTION

The Advanced Spaceborne Thermal Emission and Reflection Radiometer (ASTER) is a high-spatial-resolution multispectral imager on the Terra satellite launched in December 1999 (Yamaguchi et al., 1998). The ASTER instrument consists of three subsystems divided by spectral wavelength regions: visible and near-infrared (VNIR), shortwave infrared (SWIR) and thermal infrared (TIR) subsystems. The ASTER TIR subsystem has five spectral bands (bands 10 to 14) in the TIR spectral region (8 to 12 μm) with a spatial resolution of 90 m. These TIR bands allow the retrieval of both surface temperature and spectral emissivity which can be used in a wide variety of studies such as environmental monitoring, geological mapping and hazard prediction. In the ASTER Project, these surface parameters are generated from at-sensor radiances by the standard algorithms of atmospheric correction (Palluconi et al., 1999) and temperature/emissivity separation (TES) (Gillespie et al., 1998) on demand by a user through web sites (e.g., <http://imsweb.aster.ersdac.or.jp/>), and delivered to the user as standard products.

In general, surface emissivity retrieval is sensitive to input radiance errors, because a

dynamic range of Earth surface emissivity is not large in the TIR region: a typical dynamic range of emissivity is roughly 0.90–0.99, while some silica-rich materials can have an emissivity range of about 0.6–0.8 in a part of the TIR region. Input errors giving impacts to emissivity retrieval will be caused not only from a radiometric calibration error and an atmospheric correction error but also from a geometric correction error. It is known that some of ASTER emissivity products, particularly resampled by the nearest neighbor (NN) method, include stripe noises due to geometric correction or resampling in level-1 processing (see the ASTER GDS web site). Although this cause is uncertain, it is reported that these noises are equivalent to about 5–10% in emissivity. In the present study, we investigate the impact of band-to-band misregistration on emissivity products and suggest a geolocation approach for reducing such misregistration.

2. ASTER/TIR RELATED PRODUCTS

The lowest level ASTER product delivered to a user is a level-1A (L1A) product which is an unregistered uncalibrated image product with geometric/radiometric correction coefficients and other supplemental/ancillary data (Fujisada, 1998). A level-1B (L1B) product is a registered scaled-radiance product, and a level-3A (L3A) product is an orthogonal-projection scaled-radiance product. L1B and L3A products are generated from an L1A product. All of these products include all spectral bands (bands 1 to 14). On the other hand, level-2 products are processed and delivered for each telescope (subsystem). A level-2B01 product is a registered surface-radiance product generated from an L1B product by atmospheric correction. In the case of TIR, this correction is based on radiative transfer calculation using the MODTRAN code combined with atmospheric profiles obtained from a numerical forecast system (Palluconi et al., 1999). A level-2B03 product is a registered surface-temperature product, and a level-2B04 product is a registered surface-emissivity product, which are generated from a level-2B01 product by a temperature/emissivity separation (TES) algorithm (Gillespie et al., 1998).

A band-to-band registration accuracy of an L1B product in the same telescope is better than 0.1 pixel (Iwasaki et al., 2005). This accuracy will be enough for general purposes. In geometric correction for L1B and L3A, pixels are resampled by one of the cubic convolution (CC) method, the bi-linear (BL) method, and the nearest neighbor (NN) method. The resampling method used can be selected by a user in ordering a product through the web sites. In ordering a level-2 product, all processing options for lower level products can be selected by a user.

3. TEST DATA

In the present study, an ASTER scene acquired around Tonopah in Nevada, USA, on 26 August 2005 was used. This area is covered by mainly exposed rocks or soils, partly vegetation under a semi-arid condition. Figures 1, 2, and 3 display the VNIR image (RGB=bands 3, 2, 1), the

normalized difference vegetation index (NDVI) image calculated with bands 2 and 3, and the digital elevation model (DEM) generated from the GTOPO30 DEM product. As shown by these figures, most of vegetated surfaces are mainly located in mountainous areas. Figure 4 displays the observed radiance image of band 10 (TIR) generated from an L1B product resampled by NN. Higher elevation areas and vegetated areas show a larger radiance than other areas due to higher surface temperature.

4. IMPACT OF BAND-TO-BAND MISREGISTRATION ON EMISSIVITY

Figure 5 gives a comparison of the surface emissivity images (RGB=bands 14, 12, 10) retrieved from L1B products resampled by NN (left) and by BL (right). This retrieval was made by our software compatible with the standard atmospheric correction and TES software. The NN-based emissivity image shows significant stripe noises in mountainous areas, probably because some bands of a pixel look high temperature surfaces (sunny side) and other bands of that pixel look low temperature surfaces (shade side) due to band-to-band misregistration. The BL-based emissivity image does not show such type of noises, probably because a smoothing effect by BL reduced the misregistration effect mentioned above.

Figure 6 gives a comparison of the surface emissivity images (RGB=bands 14, 12, 10) retrieved from five kinds of observed radiance products for an area shown by a black box on Figure 5. The first emissivity image (1) was generated from an L1B product resampled by NN. Significant stripe noises can be seen as mentioned above. The second (2) was generated from an L1A product which is not geolocated. Although the maximum deviation of pixel positions among bands will be about one pixel in the cross track direction on an L1A scene, the retrieved emissivity image does not show significant noises. The third (3) was generated from an L3A orthogonal projection product, which shows a different type of stripe noises from the case (1). The fourth (4) and the fifth (5) were generated from L1A products geolocated by NN using ground control point (GCP) tables included in the L1A products. The GCP table of each band includes latitude/longitude values at lattice points (each block size is 72 x 70 pixels) (Fujisada, 1998). For the fourth emissivity image, the GCP table of each band was applied to that band, which is the same approach with L1B and L3A processing. This image demonstrates similar noises to L3A. For the fifth emissivity image, the GCP table of band 10 was applied to all bands. Although the cross-track deviation of pixel positions in an L1A product is not corrected in this case, this emissivity image as well as the case (2) shows higher quality than the cases (1), (3), and (4). This is also shown by Table 1 giving statistical emissivity values (the mean, the standard deviation, and the minimum) of bands 10–14 for a test area of 100 x 100 pixels on each emissivity image. The test area is covered by mainly vegetation which has a flat emissivity spectrum near unity. The mean emissivity is almost similar among the five cases, but the cases (2) and (5) show better results (smaller standard deviations and larger minimum emissivities) than the other cases. These results indicate that L3A products as well as L1B products include

band-to-band misregistration giving some impacts to emissivity products probably due to some mismatch in GCP tables among bands. The reason why the cases (2) and (5) include the cross-track deviation of pixel positions among bands but show less noises will be because these cases are free from mixing of pixels between different scan lines which will occur in the other cases (1, 3, and 4). If an L1A product is geolocated by a combination of cross-track matching and a single GCP table, the quality of spectral emissivity products may be improved. This will be investigated in the near future.

5. CONCLUSION

In the present study, the impact of band-to-band misregistration on emissivity products was investigated using various observed radiance products. It is well known that some of L1B products resampled by NN will produce stripe noises on emissivity products, but the results indicate that L3A products resampled by NN also will produce some stripe noises although the noise pattern is not same between L1B and L3A. We think that this cause will be in some mismatch in GCP tables among bands. L1B/L3A products resampled by BL do not show significant noises, but NN will be an important resampling method for some applications. If an L1A product is geolocated by a combination of cross-track matching and a single GCP table, the quality of spectral emissivity products may be improved even if NN is used. This will be investigated in the near future.

REFERENCES

- [1] ASTER Ground Data System (GDS), Service Center, Release Note, http://www.gds.aster.ersdac.or.jp/gds_www2002/service_e/release_e/set_release_e.html
- [2] Fujisada, H., ASTER level-1 data processing algorithm, 1998. *IEEE Trans., Geosci. Remote Sens.*, 36 (4), pp. 1101–1112.
- [3] Gillespie, A., Rokugawa, S., Matsunaga, T., Cothern, J.S., Hook, S., and Kahle, A.B., 1998. A temperature and emissivity separation algorithm for Advanced Spaceborne Thermal Emission and Reflection Radiometer (ASTER) images, *IEEE Trans., Geosci. Remote Sens.*, 36 (4), pp. 1113–1126.
- [4] Iwasaki, A., and Fujisada, H., 2005. ASTER geometric performance, *IEEE Trans., Geosci. Remote Sens.*, 43 (12), pp. 2700–2706.
- [5] Palluconi, F., Hoover, G., Alley, R., Nilsen, M.J., and Thompson, T., 1999. An atmospheric correction method for ASTER thermal radiometry over land, ASTER Algorithm Theoretical Basis Document (ATBD), revision 3, Pasadena, CA: Jet Propulsion Laboratory.
- [6] Yamaguchi, Y., Kahle, A.B., Tsu, H., Kawakami, T. and Pniel, M., 1998. Overview of Advanced Spaceborne Thermal Emission and Reflectance Radiometer (ASTER), *IEEE Trans. Geosci. Remote Sens.*, 36, pp. 1062–1071.

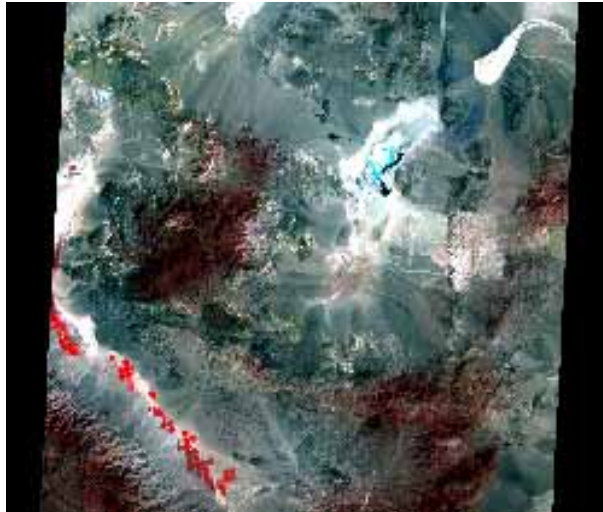


Figure 1: VNIR image (RGB=Band 3,2,1).

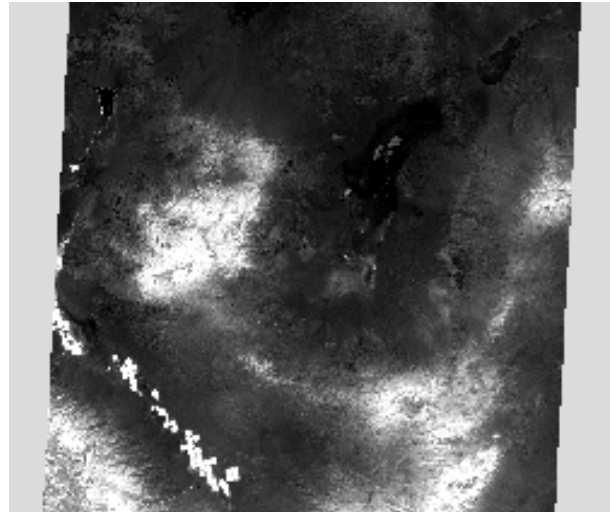


Figure 2: NDVI image derived with bands 2 and 3.

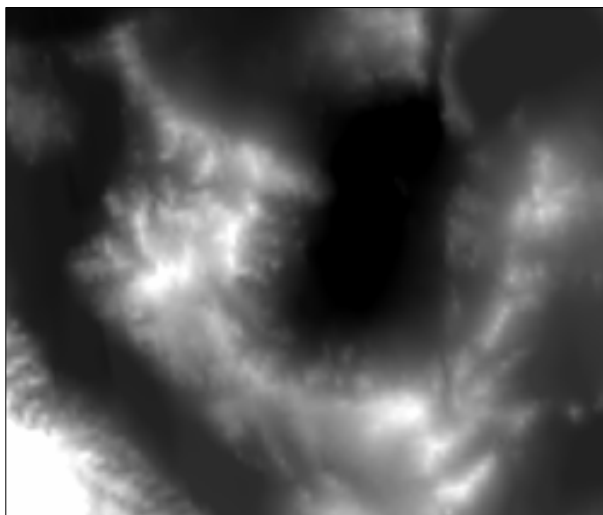


Figure 3: DEM generated from GTOPO30.

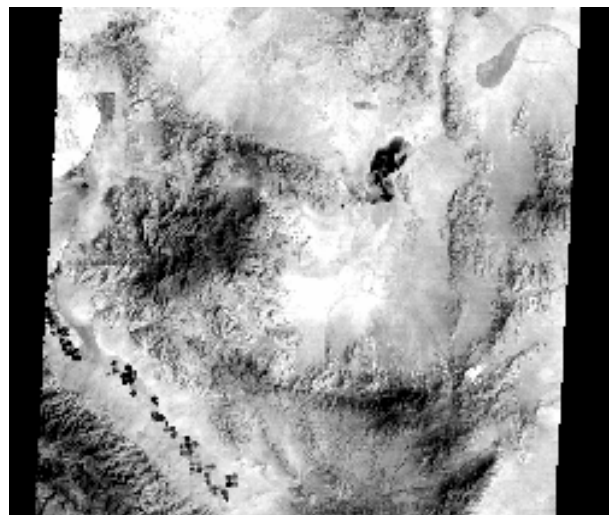


Figure 4: Observed radiance image of band 10.

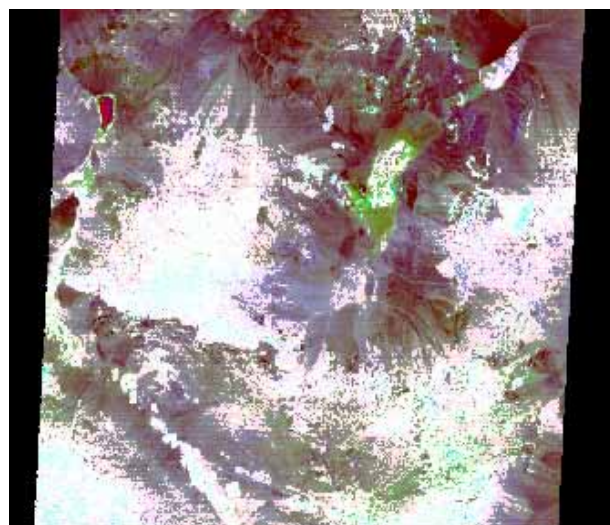
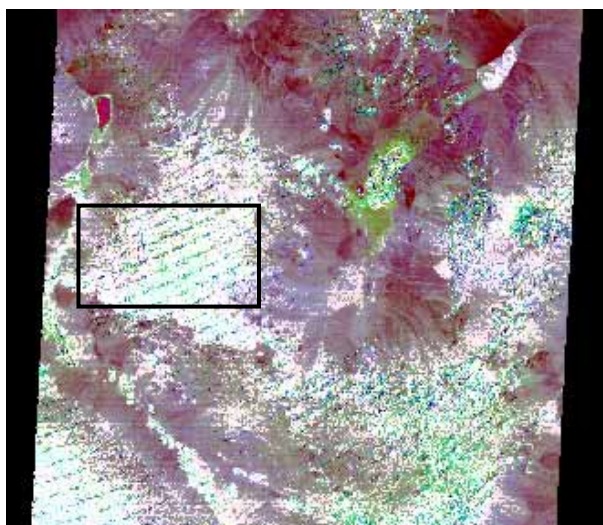


Figure 5: Emissivity images (RGB=Band 14,12,10) retrieved from L1B products resampled by NN (left) and by BL (right). A box on the left image indicates a test area used in Figure 6.

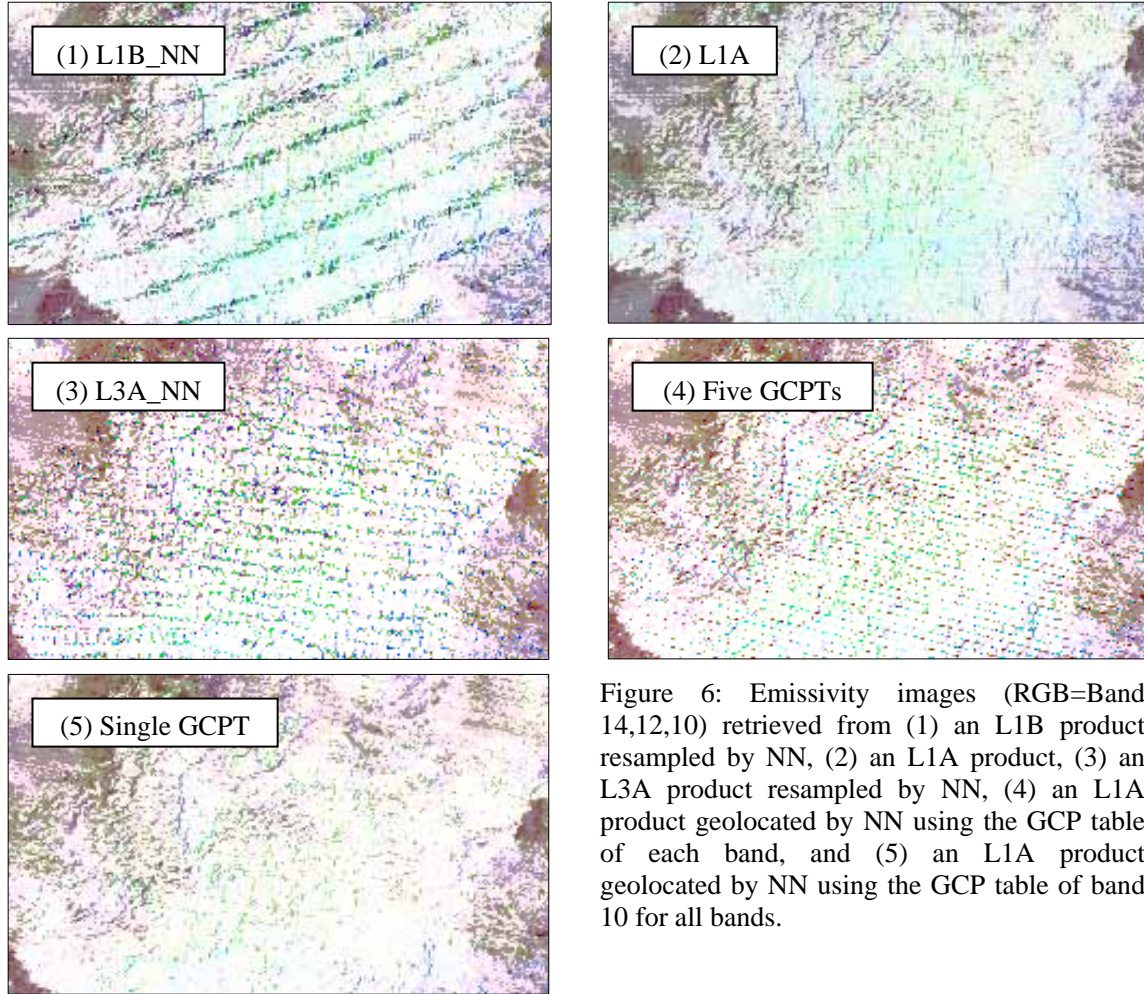


Figure 6: Emissivity images (RGB=Band 14,12,10) retrieved from (1) an L1B product resampled by NN, (2) an L1A product, (3) an L3A product resampled by NN, (4) an L1A product geolocated by NN using the GCP table of each band, and (5) an L1A product geolocated by NN using the GCP table of band 10 for all bands.

Table 1: Statistical emissivity values (the mean, the standard deviation, and the minimum) of bands 10 to 14 for a test area of 100 x 100 pixels on each emissivity image.

		L1B_NN	L1A	L3A_NN	Five GCPTs	Single GCPT
Band 10	MEAN	0.972	0.973	0.972	0.971	0.976
	STD	0.029	0.021	0.030	0.029	0.019
	MIN	0.755	0.871	0.744	0.712	0.871
Band 11	MEAN	0.977	0.978	0.975	0.975	0.980
	STD	0.023	0.018	0.026	0.027	0.016
	MIN	0.766	0.888	0.778	0.719	0.880
Band 12	MEAN	0.979	0.978	0.976	0.978	0.982
	STD	0.021	0.017	0.024	0.024	0.015
	MIN	0.808	0.885	0.818	0.746	0.885
Band 13	MEAN	0.982	0.986	0.981	0.982	0.986
	STD	0.017	0.011	0.019	0.018	0.010
	MIN	0.828	0.936	0.837	0.804	0.938
Band 14	MEAN	0.983	0.987	0.982	0.983	0.987
	STD	0.017	0.010	0.018	0.016	0.009
	MIN	0.836	0.938	0.818	0.844	0.937